

We are IntechOpen, the world's leading publisher of Open Access books Built by scientists, for scientists

6,900

Open access books available

185,000

International authors and editors

200M

Downloads

Our authors are among the

154

Countries delivered to

TOP 1%

most cited scientists

12.2%

Contributors from top 500 universities



WEB OF SCIENCE™

Selection of our books indexed in the Book Citation Index
in Web of Science™ Core Collection (BKCI)

Interested in publishing with us?
Contact book.department@intechopen.com

Numbers displayed above are based on latest data collected.
For more information visit www.intechopen.com



Detoxification of Carcinogenic Dyes by Noble Metal (Ag, Au, Pt) Impregnated Titania Photocatalysts

Sivakumar Thiripuranthagan and Valentine Rupa

Abstract

Textile industries produce large quantities of waste water which is notoriously known to contain strong colour, suspended solids and COD. Although several treatment processes, such as filtration, coagulation, oxidation, ozonation, reverse osmosis, etc., have been practiced for many decades, they all have inherent limitations. They transfer the harmful pollutants from one phase to another and do not address detoxification. Semiconductor photocatalysis is a promising technique for photodegradation of hazardous chemicals found in waste waters. Among various semiconductors, TiO_2 has been studied widely. However, the main drawbacks associated with TiO_2 are (i) large band gap ($E_g > 3.2 \text{ eV}$) (only UV active) and (ii) recombination of excitons. Dye sensitisation, coupling of semiconductors, and transitional metal doping are some of the methods reported to shift its optical response to visible region. Herein, nanoparticles of different noble metals such as Ag, Au and Pt were deposited on synthesised TiO_2 , characterized by XRD, TEM, FT-IR, BET, UV-Vis and AAS and were subjected to the degradation of some textile dyes namely Tartrazine (TAZ), Reactive Yellow-17 (RY-17) and Reactive Black-5 (RB-5) under both UV and visible irradiations. The reaction conditions such as catalyst concentration, dye concentration, pH, irradiation time, light intensity, and additives were optimized for complete decolourisation and discussed.

Keywords: photocatalyst, gold impregnated titania, textile effluent, detoxification, carcinogenic dyes

1. Introduction

Dyeing and finishing processes are the two important steps in textile industries. Large number of synthetic dyes are used extensively in the textile dyeing process and these industries produce large quantities of waste water containing carcinogenic dyes. When ground water mixes with such waste water it gets polluted and cause allergy, damage of eye, brain, liver and reproductive organs and deformities in babies during pregnant period. Thus, water pollution is a major concern in the developing nations. Though dyes are aesthetic pollutants by nature of their colour,

they may interfere with light penetration in the receiving water bodies thereby disturbing the biological processes.

Among the various types of dyes, reactive dyes are extensively used for dyeing cotton fabrics and hence they add a lot to water pollution. The volume of textile effluent discharged from dyeing industries mainly using reactive dyes are approximately calculated to be 3,00,000–4,00,000 L ton⁻¹ fabric materials in a year [1].

The increased public concern and the stringent international environmental standards have prompted the need to develop novel treatment methods for converting dye effluents to harmless compounds. Although some conventional treatment technologies such as filtration, coagulation, flocculation etc. have been tried in the past they are not viable and green technologies. Zero generation of sludge and complete mineralisation of dyes are the two important criteria for the technology to be economically attractive and environmentally benign. In this context the present study of dye treatment by using photocatalysts which mineralises the carcinogens into CO₂, H₂O and mineral salts assumes great significance.

The ideal photocatalyst should be stable, inexpensive, non-toxic and highly photoactive. Another primary criteria for the degradation of organic compounds is that the redox potential of the H₂O/OH[•] couple lies within the band gap of the semiconductor [2]. Several semiconductors have band gap energies sufficient for catalysing wide range of chemical reactions. These include TiO₂, WO₃, SrTiO₃, ZnO, ZnS, etc. Binary metal sulphide semiconductors such as CdS, CdSe and PbS are not sufficiently stable catalysts in aqueous media as they readily undergo photoanodic corrosion [3]. These materials are also known to be toxic. The iron oxides are not suitable semiconductors as they readily undergo photocathodic corrosion [4]. ZnO is unstable in water as Zn(OH)₂ being formed on the particle surface. This results in catalyst deactivation [5]. However, the anatase form of TiO₂ seems to be the best. The photoactivity of TiO₂ is known for approximately 60 years and investigated extensively. Although TiO₂ absorbs only approximately 5% of the solar light reaching the surface of the earth, it is the best-investigated semiconductor in the field of chemical conversion and storage of solar energy. Accordingly, many efforts have been made to sensitise titania for visible light induced photocatalytic reactions. Such sensitization techniques include (i) Doping with intervalent ions, (ii) heterojunctioning with other semiconductors, (iii) dye sensitization (iv), deposition of noble metals over semiconductors etc.

Herein we report the deposition of noble metals such as Au, Pt and Pd over synthesised titania. Noble metal is important because of their own catalytic activity and they actually modify the photocatalytic properties of the semiconductor by changing the distribution of electrons. Further, it can enhance the yield of a particular product or the rate of the photocatalytic reaction. The addition of a metal to a semiconductor surface also changes the reaction products. On the other hand, the loading level is important in governing the net effect of metallation as heavy metal loading induces faster electron-hole recombination [6]. One of the main reasons for the numerous studies of titania-supported metal catalysts is the so-called strong metal-support interaction (SMSI). The platinised titania exhibits a much higher activity in a series of photocatalytic reactions than pure anatase. Combined Pt-RuO₂/TiO₂ catalysts are the most promising ones for photocatalytic water cleavage [7]. The Au, Ag and Pd impregnated titania catalysts were synthesised, characterised by various instrumental techniques and evaluated towards the decolourisation of one azo dye tartrazine (TAZ) and two reactive dyes Reactive Yellow and Reactive Black (RY-17 and RB-5) (**Table 1**).

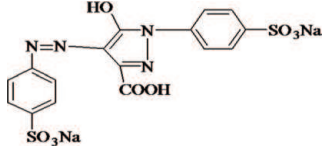
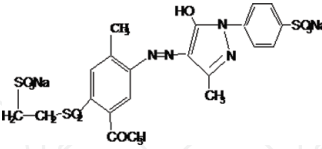
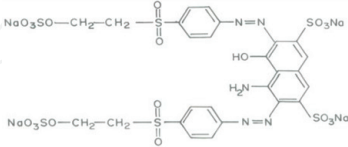
Name of the dye	Molecular Formula	Structure
Tartrazine (TAZ) Molecular Weight-534.3 λ_{\max} (nm) - 455 Dye Type- Azo C I No- C.I.19140	$C_{16}H_9N_4Na_3O_9S_2$	
ReactiveYellow-17(RY-17) Molecular Weight-691.1 λ_{\max} (nm) - 420 Dye Type- Reactive C.I No18852	$C_{21}H_{17}N_4K_2O_{10}S_3$	
Reactive Black-5 (RB-5) Molecular Weight-927.4 λ_{\max} (nm) - 597 Dye Type-Reactive C.I.20502	$C_{26}H_{21}N_5Na_4O_{19}S_6$	

Table 1.
Physicochemical properties of various dyes under study.

2. Materials and methods

2.1 Materials

Textile dyes namely Tartrazine (TAZ), Reactive Yellow-17 (RY-17) and Reactive Black (RB-5) were procured from Bagmul Sons, India and was used without any further purification.

The anatase form of TiO_2 (P-25 Degussa) with particle size 30 nm and surface area $50\text{ m}^2\text{ g}^{-1}$ was used as such. The precursors for titania, Ag, Au and Pt were titanium isopropoxide (Lancaster >99% pure), Silver nitrate (Merck >99% pure), Chloroauric acid (Merck >99% pure) and tetraammineplatinum (II) chloride (Merck >99% pure) were used as received.

All other chemicals namely NaCl, C_2H_5OH , Na_2CO_3 , H_2O_2 , $K_2S_2O_8$, NH_4OH , H_2SO_4 , isopropanol and acetic acid were obtained from Merck (purity >98%) and were used as received. The water employed for the studies was doubly distilled.

2.2 Synthesis of photocatalysts

The catalytic materials used in the present study were synthesised as described below:

2.2.1 Synthesis of TiO_2

Sol gel process was adopted for the synthesis of TiO_2 . Titanium isopropoxide, isopropanol, water and acetic acid were used as starting materials. Solution A contained 17 mL titanium isopropoxide and 40 mL of isopropanol and Solution B contained 60 mL of isopropanol, 15 mL acetic acid and 5 mL water. Solutions A and B were mixed and stirred for 2 h. The formed TiO_2 sol was aged to get the gel of TiO_2 . The obtained gel was dried, ground with mortar and pestle and finally calcined at 500°C for 3 h [8].

2.2.2 Synthesis of M/TiO_2 ($M = Ag, Au$ and Pt)

The M/TiO_2 ($M = Ag, Au$ and Pt) catalysts were prepared by photoreduction method [9]. Calculated amounts of noble metal precursors (0.14 g of $AgNO_3$ for 1%

Ag/TiO₂, 0.15 g of AuCl₃ for 1% Au/TiO₂, 0.14 g of [Pt(NH₃)₄]Cl₂ for 1% Pt/TiO₂) taken in minimum amount of water was added to 10 g of synthesised TiO₂ and was stirred at 70°C till the evaporation of the solvent. The colloidal solution was then irradiated with 125 W halogen lamp until complete reduction was observed visually by the formation of black precipitate for Ag/TiO₂, Pt/TiO₂ and purple coloured product for Au/TiO₂.

2.3 Characterisation of the catalysts

2.3.1 X-ray diffraction analysis

Synthesised TiO₂ and M/TiO₂ photocatalyst were subjected to powder X-ray diffraction to confirm the crystalline size and the presence of the metal ion. The powder X-ray diffractograms were recorded using a X-ray diffractometer (PANalytical X'Pert Pro) with Cu K α source having wavelength of 1.54 Å operating at 20 mA and 50 kV. The samples were scanned from 0.5–80° (2 θ) for the confirmation of phase and presence of metal particles. The diameter of the metal particles was calculated from the (111) reflection of metal atom using Debye Scherrer equation,

$$d = K\lambda/\beta \cos \theta \quad (1)$$

where d, diameter of the metal particle; K, constant; λ , wavelength of the X-ray (1.54 Å); β , full width at half maximum; θ , angle of diffraction.

2.3.2 Transmission electron microscopy

Particle size of the noble metals deposited on TiO₂ was determined from electron micrographs taken by using transmission electron microscope (JEOL JEM-2010F) operating at 200 kV. A drop of alcoholic solution of the catalysts was placed on Cu grid and kept aside for about 45 s. Then transmission electron micrographs were recorded for the particles present on the grid. From the TEM images, average particle size of the catalysts was determined by taking minimum of 30 particles.

2.3.3 BET surface area analysis

BET surface area analyser (Nova-Quantachrome 4200 e) was used to measure the surface area of all the catalysts. The measurement was done by using N₂ as probe molecule at liquid nitrogen temperature (–190°C). Before the measurement, all the catalysts were degassed at 300°C at the pressure of 10^{–5} Torr for 6 h. Linear portion of the BET plots was used for the determination of BET surface area.

2.3.4 Atomic absorption spectroscopic studies

The actual amount of metal content present in the synthesised catalysts (M/TiO₂, M = Ag, Au and Pt) was determined using atomic absorption spectrophotometer (Perkin Elmer 2380) after digesting the photocatalysts in aqua regia.

2.3.5 UV-visible spectrophotometry

UV-visible spectra of all the samples were recorded using UV-Vis double beam spectrophotometer (Hitachi U-2000) in the range 200–800 nm. The course of

reduction of noble metal ions on TiO₂ particles and extent of decolourisation were studied using this technique. Further, the band gap energies (E_g) of the synthesised catalysts were calculated according to the equation

$$E_g = h c / \lambda \quad (2)$$

where h, Planck's constant; c, velocity of light (m/s); λ , wavelength (nm).

2.4 Photodecolourisation studies

2.4.1 Preparation of synthetic dye samples

Stock solutions (10⁻⁴ M for TAZ and 10⁻⁵ M for both RY-17 and RB-5) of the dye samples were prepared for the present study.

2.4.2 Batch photocatalytic reactor

The photocatalytic reactor was made up of quartz having dimensions 30 × 3 cm (height × diameter) provided with water circulation arrangement to maintain the temperature. The top portion of the reactor has ports for sampling.

The irradiation was carried out using low pressure mercury arc lamp (wave length 254 nm) as UV source and tungsten lamp (365 nm) as visible light source built into a lamp housing with polished anodised aluminium reflectors placed 6.5 cm away from the lamps. The entire reactor system was cooled using an inbuilt fan set up.

2.4.3 Photocatalytic reaction

250 mL of the desired dye sample was taken in a photocatalytic reactor. Calculated amount of TiO₂ (P-25 Degussa) or synthesised TiO₂ or M/TiO₂ was added to the photocatalytic reactor and the reaction mixture was magnetically stirred before and during illumination. After specific time interval of irradiation, suitable aliquots of the sample was withdrawn and analysed to find out the extent of decolourisation and degradation.

2.4.4 UV-vis analysis of the decolourised products

The extent of photocatalytic decolourisation of dyes was studied by UV-visible spectrophotometer (Hitachi U-2000) from the decrease in the respective λ_{\max} values.

The colour intensity of the dyes was measured in terms of absorbance. Decolourisation was determined by using the calibration curve.

$$\text{Decolourisation (\%)} = \frac{C_0 - C}{C} \times 100 \quad (3)$$

where C₀, initial concentration of the dye; C, concentration of dye at time 't'.

2.5 Photodegradation studies

The photocatalytic degradation of dyes was evaluated in terms of total organic carbon (TOC). The total organic carbon of the pollutant was determined by using a TOC analyser (Shimadzu TOC V series).

2.6 Textile effluent study

To check the photocatalytic activity of M/TiO₂ catalyst for the photocatalytic degradation of actual textile effluent, the samples were collected from M/s Ramkay & Co, Erode, Tamil Nadu, India, filtered and diluted. Since the effluent contains number of unknown dyes it gave a broad peak in the wavelength range of 500–600 nm. Since the absorbance is additive, the effluent simply shows a broad peak in this range. To the diluted effluent (250 mL), 6 g of M/TiO₂ (M = Ag, Au and Pt) catalyst was added and the photocatalytic study was performed in the photocatalytic reactor.

2.6.1 COD experiment

Chemical oxygen demand (COD) of the samples collected at different intervals was determined by dichromate method in the presence of a catalyst Ag₂SO₄ [10, 11].

3. Results and discussion

3.1 Characterisation of synthesised TiO₂ and M/TiO₂ photocatalysts

3.1.1 UV-visible spectrophotometry

The absorption spectra of synthesised TiO₂ (gel form) was recorded using UV-visible spectrophotometer and given in **Figure 1**. An absorption maxima observed around 320 nm is due to the charge transfer from the VB of 2p orbitals of the oxide ions to the CB of 3d_{t2g} orbitals of the titania cations [12].

The optical absorption evolution spectra of solutions of noble metal precursors (2×10^{-3} M AgNO₃, 2×10^{-4} M HAuCl₄ and 1×10^{-5} M [Pt(NH₃)₄]Cl₂) in the presence of TiO₂ colloid during visible irradiation are shown in **Figure 1**.

This figure shows that on visible irradiation, appearance of new bands centred on 370 nm for Ag, 520 nm for Au and 502 nm for Pt were observed. The reason for

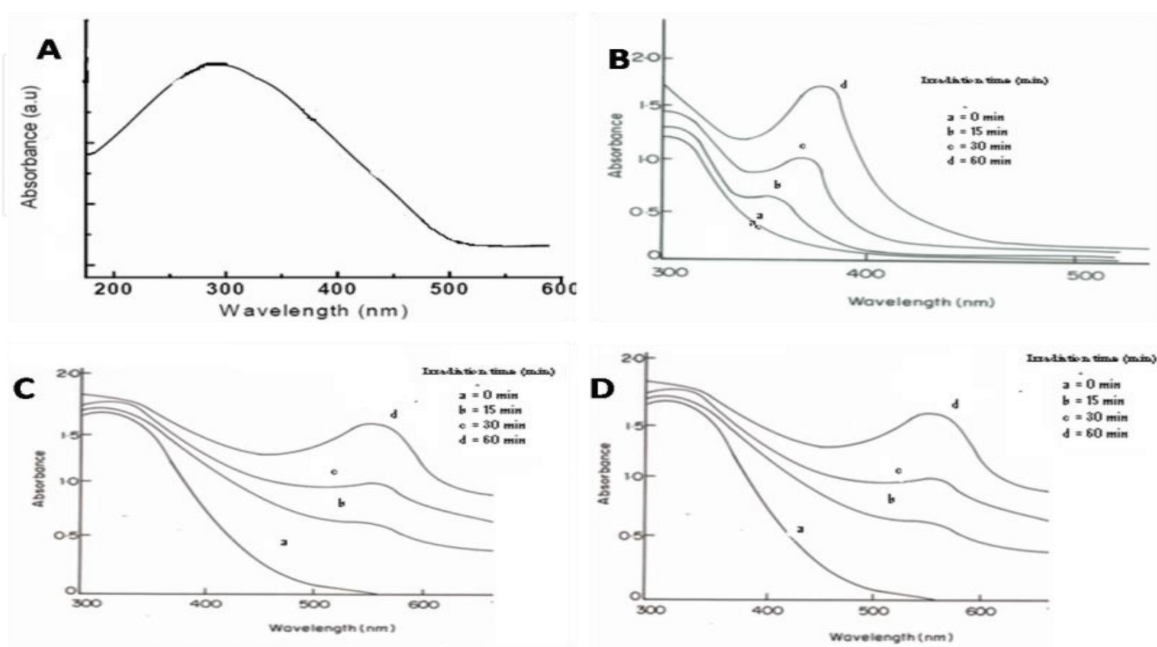


Figure 1.

(a) UV-visible spectrum of synthesised TiO₂ and optical absorption evolution spectra of (b) Ag/TiO₂ (c) Au/TiO₂ and (d) Pt/TiO₂ at different time intervals.

appearance of these peaks is due to the surface plasmon excitation of the respective metal colloids [13–15].

The band gap values of all the synthesised catalysts (TiO_2 and M/TiO_2) were calculated from the corresponding λ values obtained by extrapolating the rising portion of the spectrum to the x axis at zero absorbance and by using the following equation. The values were consistent with the values reported already [16].

$$E_g = hc/\lambda \quad (4)$$

where E_g , band gap energy; h , Planck's constant in eV (4.135×10^{-15} eV); c , velocity of light (3×10^8 m/s); λ , wavelength of corresponding M/TiO_2 catalysts 370 nm for Ag, 520 nm for Au and 502 nm for Pt.

The band gap values for the synthesised TiO_2 and metal loaded TiO_2 are given in **Table 2**. The band gap values were found to be lower for the metal loaded catalyst when compared to the synthesised TiO_2 catalyst.

Although lowering of band gap is not good for better catalytic activity under UV irradiation due to easy recombination, the presence of metals act as electrons traps and prevents the recombination process and also making the photocatalyst active in the visible range.

3.1.2 Atomic absorption spectrophotometric analysis

To determine the actual metal content of all the synthesised M/TiO_2 catalysts, they were subjected to AAS analysis after dissolving them. The metal content in each catalyst determined is given in **Table 2**. The results show that the experimentally determined metal content value is close to that of the theoretical value (1% w/w).

3.1.3 BET surface area measurements

The surface area of all the synthesised catalysts viz., TiO_2 (P-25 Degussa), TiO_2 and M/TiO_2 catalysts were determined and given in **Table 2**. **Table 2** clearly shows that the synthesised catalysts show higher surface than commercial TiO_2 (P-25 Degussa). It is to be noted that impregnation of noble metals (Pt, Pd and Au) over TiO_2 did not alter the surface area values significantly. A very small reduction in the surface area observed may be due to the blocking of fine capillaries present on TiO_2 surface by metal thin islands. These islands prevent the entry of the probe molecule (nitrogen gas) into the pores during BET measurement [17].

3.1.4 X-ray diffraction analysis

To obtain information regarding the phase formation and crystallite size, X-ray diffraction measurements were performed for the synthesised TiO_2 and M/TiO_2 ($\text{M} = \text{Ag, Au and Pt}$) photocatalysts and the XRD patterns are shown in **Figure 2**.

The synthesised TiO_2 has both anatase and rutile phases but not the brookite phase. Anatase and rutile phases are confirmed by the appearance of major peaks at $2\theta = 25.4$ and 48° respectively. The corresponding d (111) reflections of the noble metal atoms were found at $2\theta = 38.1, 38.8$ and 40° for Ag, Au and Pt, which confirms the impregnation of metal particles on TiO_2 lattice. From the X-ray diffraction patterns the average particle size of the synthesised TiO_2 and M/TiO_2 was calculated using Debye-Scherrer equation.

$$d = K\lambda/\beta \cos \theta \quad (5)$$

(A)	Catalyst	Band gap (eV)	(B)	Catalyst	Noble metal content (Wt. %)
	TiO ₂ (P-25 Degussa)	3.2		Ag/TiO ₂	0.97
	Synthesised TiO ₂	3.8		Au/TiO ₂	0.96
	Ag/TiO ₂	3.3		Pt/TiO ₂	0.98
	Au/TiO ₂	2.3			
	Pt/TiO ₂	2.4			

(C)	Catalysts	BET surface area (m ² g ⁻¹)	(D)	Catalyst	Particle Size (nm)
	TiO ₂ (P-25 Degussa)	50.2		Synthesised TiO ₂	24
	Synthesised TiO ₂	90.5		Ag/TiO ₂	11
	Ag/TiO ₂	87.3		Au/TiO ₂	10
	Au/TiO ₂	88.1		Pt/TiO ₂	19
	Pt/TiO ₂	87.8			

Table 2. Physicochemical characteristics of bare and M/TiO₂ catalysts.

where d, diameter of the metal particle; λ , wavelength of the X-ray radiation ($\lambda = 0.15418 \text{ nm}$), $K = 0.98$ (constant); θ , characteristic X-ray diffraction peak; B = full width at half maximum in radians.

The average particle diameter of the synthesised TiO₂ and M/TiO₂ was found to be in the nanometre range as shown in Table 2.

3.1.5 Transmission electron microscopy

TEM images and particle size histograms of synthesised TiO₂, Ag, Au and Pt deposited TiO₂ catalysts are shown in Figure 3. Almost uniform dispersion was obtained

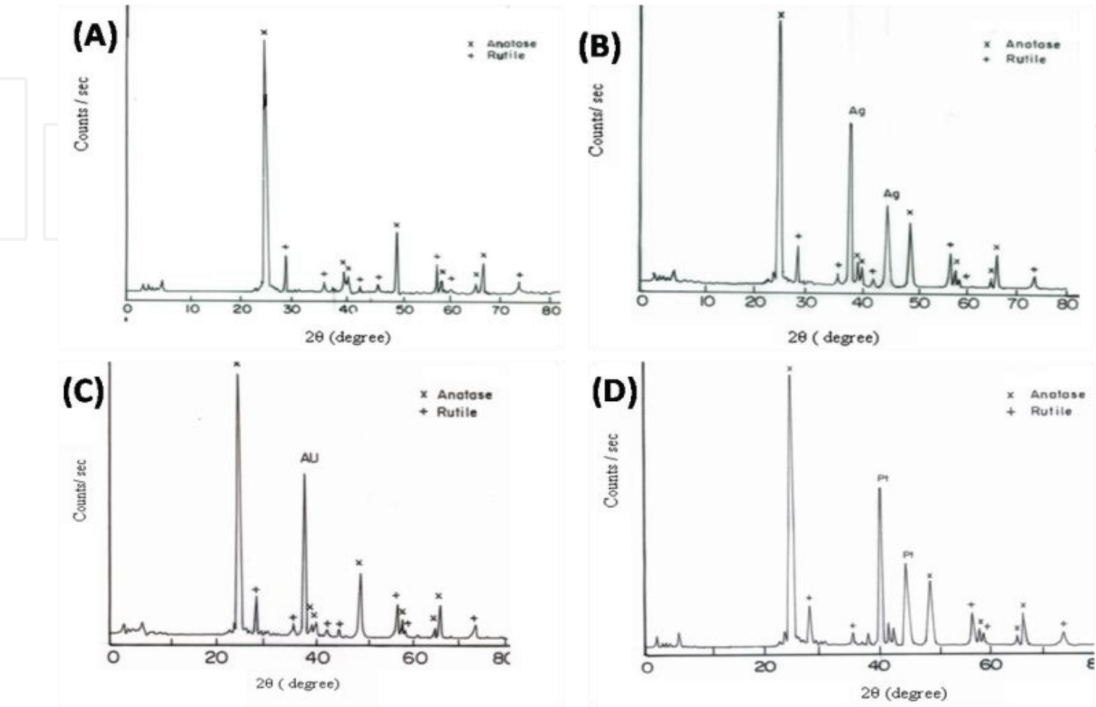


Figure 2. X-ray diffraction patterns of (A). synthesised TiO₂, (B). Ag/TiO₂, (C) Au/TiO₂ and (D). Pt/TiO₂.

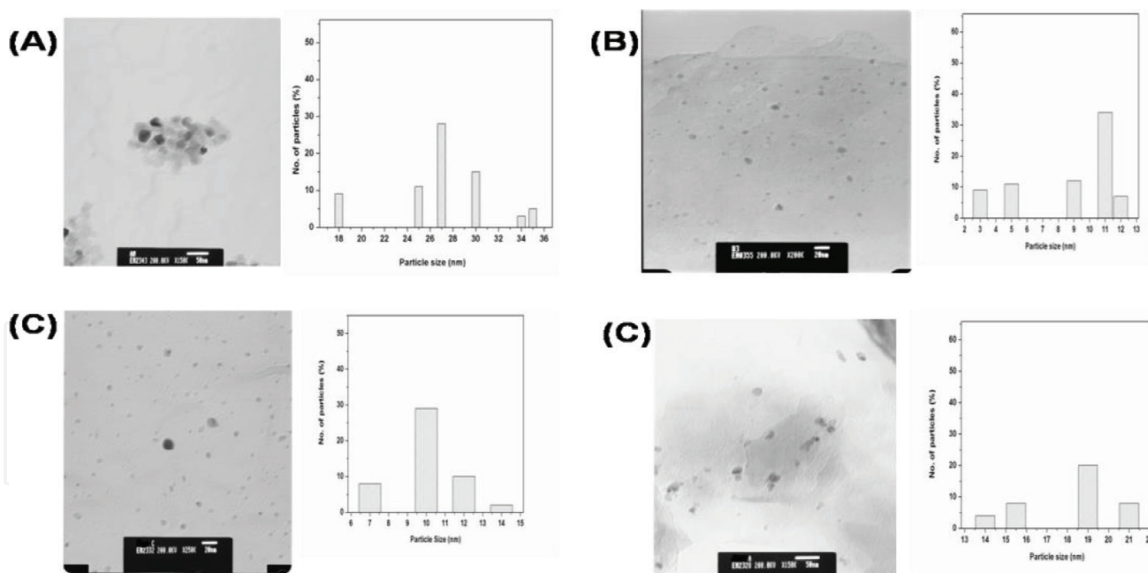


Figure 3.
Transmission electron micrograph and particle size histograms of (A) synthesised TiO_2 , (B) Ag/TiO_2 , (C) Au/TiO_2 and (D) Pt/TiO_2 .

with all the catalysts. The average size of the particles was calculated by averaging particle sizes of 20–30 particles. The plot of particle size distribution is also shown.

The average particle size of TiO_2 , Ag/TiO_2 , Au/TiO_2 and Pt/TiO_2 catalyst was found to be 27 nm, 11 nm, 10 nm and 19 nm respectively.

3.2 Photocatalytic studies on TiO_2 (P-25 DEGUSSA)

3.2.1 Effect of initial concentration of dye

The effect of initial concentration of dye on the rate of decolourisation was studied by taking 250 mL of dye solutions and varying the concentrations between 8×10^{-5} and 1.3×10^{-4} M for Tartrazine (TAZ), 8×10^{-6} and 1.6×10^{-5} M for RY-17 and 6×10^{-6} and 1.6×10^{-5} for RB-5 with constant catalyst weight (1.5 g). The irradiation was carried out for 6 h by using 125 W low pressure mercury arc lamp (wave length 254 nm) and 85 W tungsten lamp (wave length 365 nm) as UV and visible light sources, respectively. **Figure 4** shows that percentage decolourisation decreases as the initial concentration of the dye increases under both UV and visible light illumination.

Similar results in the photocatalytic degradation of phenol were reported in the literature [18, 19]. The decolourisation rate relates to the probability of formation of hydroxyl radicals (OH^\cdot) on the catalyst surface and the probability of hydroxyl radicals reacting with dye molecules. Hence the rate constant depends on the probabilities of the formation of these two. Hence k' can be expressed as

$$k' = k_0 \times P_{\text{OH}^\cdot} \times P_{\text{dye molecules}} \quad (6)$$

where k' is the overall rate constant and k_0 is the reaction rate constant. P_{OH^\cdot} and $P_{\text{dye molecules}}$ refer to the probabilities of generation of OH^\cdot radicals and OH^\cdot radicals reacting with dye molecules. We all know that the reaction rate constant k_0 is independent of initial dye concentration but P_{OH^\cdot} and $P_{\text{dye molecules}}$ will be affected by the dye concentration. Literature suggests that photocatalytic degradation of aromatic compounds mainly occurs by hydroxyl radicals [20]. The rate determining step of the reaction may be the formation of OH^\cdot radicals that are formed through the reaction of holes with adsorbed OH^- and H_2O [21, 22].

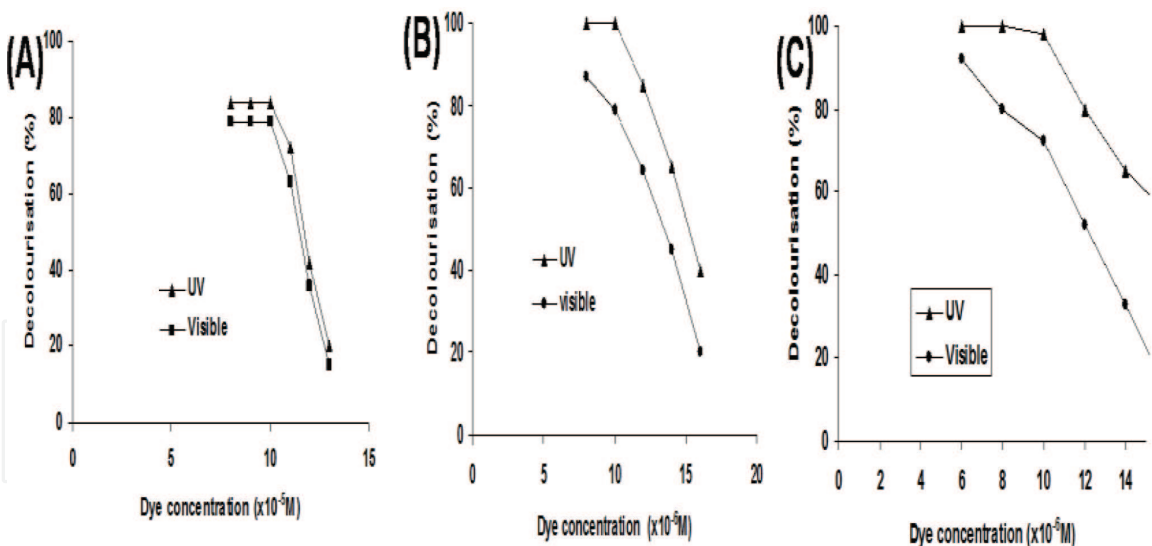
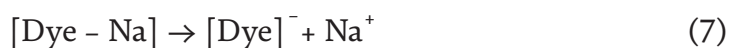


Figure 4.

Effect of initial concentration of (A) TAZ, (B) RY-17 and (C) RB-5 dyes on the % decolourisation under UV and visible irradiations. (reaction conditions: Weight of catalyst (P-25 Degussa) = 1.5 g, volume of dye solution = 250 mL, irradiation time = 6 h (UV): 6 h (visible) and pH = neutral).

As the dye concentration increases, the available hole sites may be occupied by dye ions which are generated from the sodium salt of the dye molecules,



Since there are only a few active sites available for the generation of OH^\cdot radicals the generation of OH^\cdot will be reduced.

It is concluded that as the initial dye concentration increases, the catalyst surface needs to generate more amount of OH^\cdot radicals and other oxidising species. But, illumination time and required amount of the catalyst are constant, so that OH^\cdot radicals and other oxidising species formed on the TiO_2 surface are also constant. So the relative number of OH^\cdot attacking the dye molecules decreases with increasing dye concentration [23]. Moreover, as the initial concentration of the dye increases, the path length of photons entering the solution decreases and at low dye concentration the reverse effect is observed [24, 25]. Also, at higher concentration, degradation decreases at sufficiently long distances from the light source or reaction zone due to retardation in the penetration of light. Hence, under both UV and visible light sources the rate of degradation decreases considerably with increase in dye concentration above the optimal concentration.

3.2.2 Effect of catalyst weight

A series of experiments were carried out to assess the optimum weight of the catalyst by varying the amount of TiO_2 (P-25 Degussa) from 0 to 3 g for the decolourisation of 250 mL of dye solution (TAZ = 1×10^{-4} M, RY-17 and RB-5 = 1×10^{-5} M) at the irradiation time of 6 h at neutral pH. The effects of catalyst weight on the percentage decolourisation of all the dyes are shown in **Figure 5**.

In the absence of the catalyst no decolourisation occurred. From the figure it is also evident that the rate of photodecolourisation increased linearly with the weight of catalyst up to 1.5 g irrespective of light sources. On increasing the catalyst weight further, the percentage decolourisation decreased. This decrease in decolourisation on increasing the catalyst weight may be due to the formation of turbidity (Shadowing effect). Similar observation was also reported [26]. Optimum catalyst

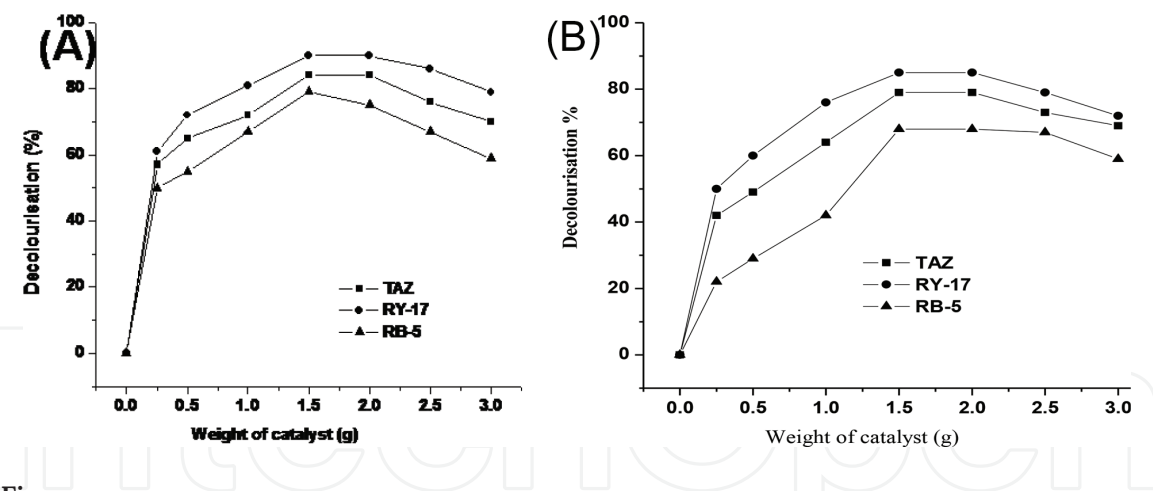


Figure 5. Effect of weight of catalyst on the decolourisation of dyes under (A) UV and (B) visible irradiations (reaction conditions: Dye concentration: TAZ = 1×10^{-4} M, RY-17 = 1×10^{-5} M, RB-5 = 1×10^{-5} M, volume of dye solution = 250 mL, irradiation time = 6 h and pH = 7).

loading is always essential and the higher amount of TiO_2 may not be useful both in view of aggregation as well as reduced irradiation field due to shadowing effect [27].

As the weight of the catalyst increased, the quantity of photons adsorbed increased and consequently the decolourisation rate increased [28], Hence, optimisation of the catalyst loading for a given dye concentration is an important parameter to avoid excess catalyst and to ensure total absorption of light either UV or visible light for efficient photodecolourisation.

3.2.3 Effect of pH

The effect of pH on decolourisation of dyes irradiated under UV and visible irradiation are given in **Figure 6**.

The percentage decolourisation of all the dyes was found to be maximum at the pH of 7 for UV and visible irradiations. On increasing the pH from acidic to neutral under UV and visible irradiations, the percentage decolourisation increased significantly. However, when the pH was increased beyond these values to the basic ranges the percentage decolourisation decreased drastically. The main reaction is presented by the hydroxyl radical attack on the dye anion. Hydroxyl radicals

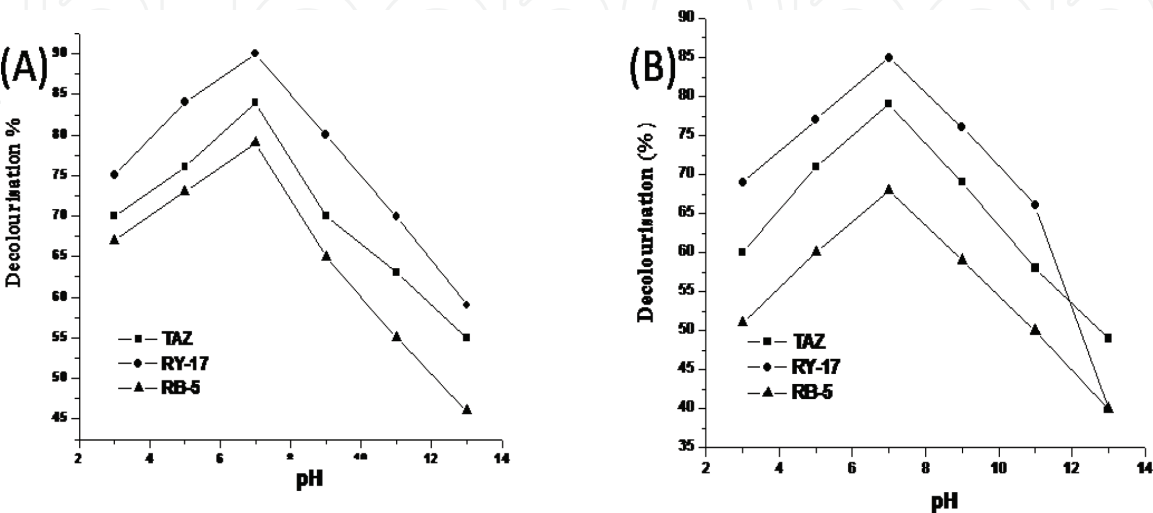


Figure 6. Effect of pH on decolourisation of dyes under (A) UV and (B) visible irradiations (reaction conditions: Dye concentration: TAZ = 1×10^{-4} M, RY-17 = 1×10^{-5} M, RB-5 = 1×10^{-5} M, volume of dye solution = 250 mL and irradiation time = 6 h).

which are considered as the predominant species at neutral or alkaline pH values are generated by oxidising more hydroxide ions [29]. At low pH values ($\text{pH} < 5$) the photodecolourisation of dyes is retarded under both UV and sunlight sources by the high concentration of the proton. Lack of availability of hydroxyl radicals in the pH range less than 5 leads to the decrease in decolourisation of dyes. In highly alkaline conditions ($>\text{pH} 9$) the % decolourisation of dyes decreased drastically due to the electrostatic columbic repulsion between the anionic dye surface (negatively charged) and the hydroxyl anions. Due to this repulsion, the dyes do not interact closely with the anions [30–33]. Thus it is deduced that the efficient condition for the maximum degradation of all the mentioned dyes is at neutral pH ($\text{pH} = 7$).

3.2.4 Photocatalytic degradation studies

The extent of degradation of dyes was followed by total organic carbon analyser (TOC). The experimental results revealed that as the irradiation time increased, some dye molecules may degrade into components of lower molecular fragments and they mineralise. TOC analysis was carried out for all the dye samples collected at different intervals of time and the results are shown in the **Figure 7**.

Since the decrease in the TOC content is the direct measure of degradation, TOC studies have been carried out to check whether the photocatalyst converts the harmful dye into harmless products. The studies revealed that, about 45% of TOC of dye samples was reduced under UV and 35% under visible irradiations. Similar type of observations was also made by [34, 35]. The degradation of dye involved the cleavage of —N=N— and sequential evolution of N_2 in the early stage of degradation [36]. The fate of nitrogen containing compounds in the photodegradation was also explained by [37].

3.2.5 Recycling of TiO_2

In order to test the recyclability of TiO_2 catalyst, the experiment was repeated with 250 mL of dye solutions ($\text{TAZ} = 1 \times 10^{-4} \text{ M}$, RY-17 and $\text{RB-5} = 1 \times 10^{-5} \text{ M}$) with the used catalyst. The photocatalytic experiments were carried out with 1.5 g of TiO_2 (P-25 Degussa) for 5 h. At the end of reaction, the dye samples were filtered and the catalyst was filtered off. There was not much difference between the weight of the recovered catalyst with its initial weight ($<1\%$). Repeated experiments were carried out for another 5 h by taking 250 mL of fresh dye solution. The pseudo first order rate constant values were calculated for each cycle as mentioned before and the values are given in **Table 3**.

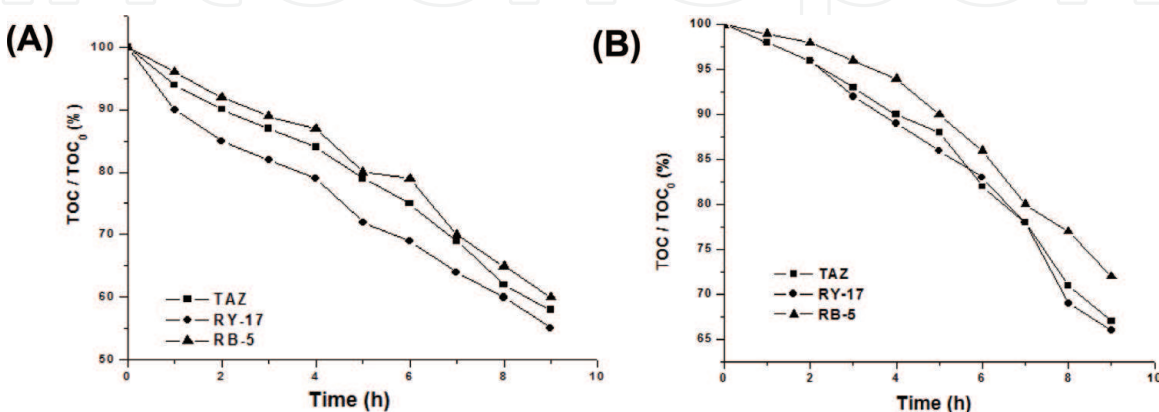


Figure 7.

Mineralisation of dyes using TiO_2 (P-25 Degussa) under (A) UV and (B) irradiations (reaction conditions: Dye concentration: $\text{TAZ} = 1 \times 10^{-4} \text{ M}$, $\text{RY-17} = 1 \times 10^{-5} \text{ M}$, $\text{RB-5} = 1 \times 10^{-5} \text{ M}$, volume of dye solution = 250 mL, irradiation time = 9 h and $\text{pH} = 7$).

No. of cycles	Pseudo first order rate constant K (min ⁻¹)					
	Tartrazine		Reactive Yellow-17		Reactive Black-5	
	UV	Visible	UV	Visible	UV	Visible
Fresh	8.7 × 10 ⁻³	7.0 × 10 ⁻³	9.4 × 10 ⁻³	8.3 × 10 ⁻³	6.3 × 10 ⁻³	5.4 × 10 ⁻³
I-recycle	8.15 × 10 ⁻³	6.9 × 10 ⁻³	9.1 × 10 ⁻³	8.1 × 10 ⁻³	5.9 × 10 ⁻³	5.2 × 10 ⁻³
II-recycle	8.09 × 10 ⁻³	6.2 × 10 ⁻³	8.2 × 10 ⁻³	7.9 × 10 ⁻³	5.3 × 10 ⁻³	4.9 × 10 ⁻³

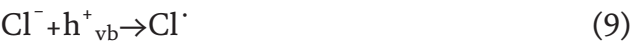
Table 3.
Effect of catalyst recyclability on the degradation of textile dyes.

The rate constant values were found to be almost the same for all the dyes under both UV and visible irradiations even after two cycles. Nevertheless at the end of II recycle, 91% decolourisation occurred in the illumination period of 5 h. This shows that the TiO₂ (P-25 Degussa) is a very good catalyst which does not undergo significant deactivation even after 2 cycles. A very slight decrease in the rate constant values obtained in the photocatalysis experiments may be due to the adsorption of dye on the active sites of the catalysts which could not be removed during filtering.

3.2.6 Effect of inhibitors

Large amount of sodium chloride is used in the dyeing process in the textile industries and hence it usually comes out in the dye effluent along with sectional water of textile mills. Sodium carbonate also plays an important role in fixing the dye on fabrics and in the fastness of colour and hence it is mainly used in the dye bath to adjust the pH of the bath. Alcohols are used for padding process during dyeing the fabrics. Alcohols such as ethanol are commonly used to quench hydroxyl radicals. Hence, it is important to study the influence of chloride ions, carbonate ions and ethanol on the photomineralisation efficiency of the catalyst. Irradiation experiments were carried out by taking 250 mL of different dyes of various concentration (TAZ = 1 × 10⁻⁴ M, RY-17 and RB-5 = 1 × 10⁻⁵ M), 1.5 g of TiO₂ (P-25 Degussa) under neutral pH and with different concentrations of (0–2 g) for both sodium chloride and sodium carbonate and 0 to 1 mL of ethanol. The irradiation was carried out by using 125 W low pressure mercury arc lamp and 85 W tungsten lamp as UV and visible light sources, respectively. The results obtained under both UV-visible irradiations are shown in **Figure 8**.

The presence of chloride ion in the dye samples had a negative effect on decolourisation. The percentage decolourisation decreased drastically with increase in the concentration of sodium chloride. This decrease in the percentage decolourisation of dyes in the presence of chloride ion is due to the hole-scavenging properties of chloride ion (equations 7 and 8).



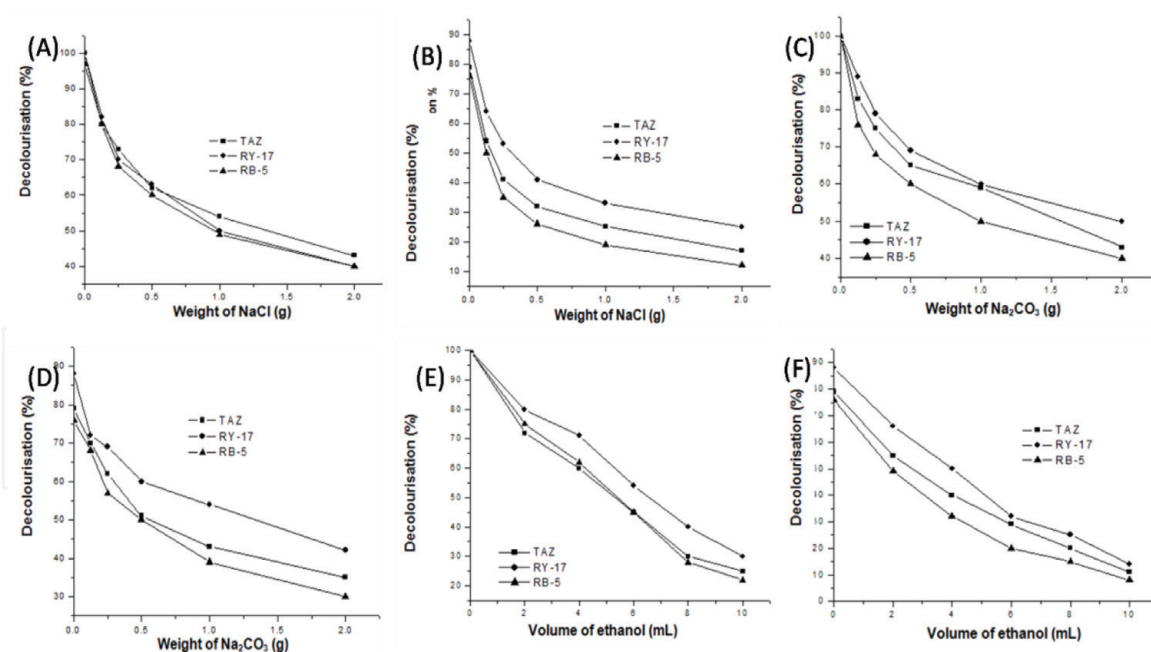
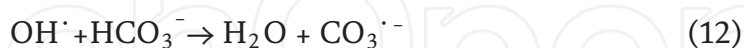
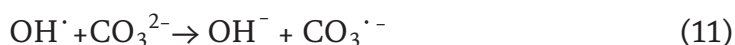


Figure 8.

Effect of (A) sodium chloride, (C) sodium carbonate and (E) ethanol on decolourisation of dyes under UV and (B, D, F) visible irradiations. (reaction conditions: Dye concentration: TAZ = 1×10^{-4} M, RY-17 = 1×10^{-5} M, RB-5 = 1×10^{-5} M, weight of catalyst (P-25 Degussa) = 1.5 g, volume of dye solution = 250 mL, pH = neutral and irradiation time = 6 or 6 ½ h).

This is a distinctive competitive inhibition reaction where the reaction of dye molecules with the holes has to compete with the chloride ions, which are not readily oxidisable. This inhibitive effect was also observed by [38]. However, the photocatalytic activity of the catalyst can be fully restored by washing the catalyst with pure water.

The decrease in the degradation of dyes in the presence of carbonate and bicarbonate ions is due to the hydroxyl scavenging property of carbonate ions according to the following Eqs. (11) and (12).



The presence of carbonate and bicarbonate ions reduces the concentration of hydroxyl radicals significantly and hence the percentage decolourisation of the dyes decreases [39].

When the volume of ethanol was increased the photodecolourisation efficiency gradually decreased. This shows that the dye degradation occurs via positive holes (h^+_{vb}) that are not involved in recombination with electrons during illumination process. Further it is evident that hydroxyl radicals are not the only species responsible for degradation and minor degradation also occurs through holes generated during illumination [40].

3.2.7 Effect of electron acceptors

The practical problem in using TiO₂ as a photocatalyst is the undesired electron/hole recombination. In the absence of proper electron acceptors or donors the electron/hole recombination is extremely efficient and represents the major energy wasting step which limits the achievable quantum yield. One strategy to inhibit

electron/hole recombination is to add other electron acceptors such as hydrogen peroxide, persulphate ions to the reaction mixture.

Hydrogen peroxide is extensively used in commercial bleaching of textiles, especially cellulose fibres and wool. In order to study the influence of hydrogen peroxide in the decolourisation of dyes, experiments were performed by adding different quantities of hydrogen peroxide (30% v/v) (0–10 mL) and 0 to 2 g of potassium persulphate to 250 mL of different dyes of various concentration (TAZ = 2×10^{-4} M, RY-17 and RB-5 = 2×10^{-5} M), 1.5 g of TiO₂ (P-25 Degussa) under neutral pH. The irradiation was carried out by using 125 W low pressure mercury arc lamp and 85 W tungsten lamp as UV and visible light sources respectively.

The presence of hydrogen peroxide will prevent the (e⁻/h⁺) pair recombination and enhances the formation of hydroxyl radicals (Eq. 13).



Since hydrogen peroxide is better than molecular oxygen as electron acceptor it leads to 100% decolourisation in comparison to the results obtained in the absence of H₂O₂. But, in the absence of TiO₂, and with only H₂O₂ the percentage decolourisation was found to be less under both the light sources as shown in **Figure 9**.

The percentage decolourisation increased on increasing the volume of H₂O₂ from 0 to 10 mL. However, percentage decolourisation decreased on increasing the volume of H₂O₂ beyond 10 mL. Since, H₂O₂ is a powerful hydroxyl scavenger, the percentage decolourisation decreased at the higher concentration as shown in Eqs. (14) and (15).



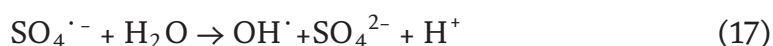
The above decolourisation results carried out by both UV and visible sources show the necessity of choosing the proper dosage of hydrogen peroxide for maximum decolourisation. Thus, it is clear from the **Figure 9** that addition of H₂O₂ up to 10 mL concentration showed a beneficial effect on the photocatalytic decolourisation of the dyes [41].

The rate of photo-assisted decolourisation of dyes is significantly improved by the presence of persulphate ions.

The percentage decolourisation increased with increase in the amount of K₂S₂O₈ and 100% degradation was attained at highest concentration of K₂S₂O₈ for both UV and visible irradiations. The added persulphate ion acts as electron traps resulting in the formation of reactive radical intermediate SO₄^{•-} as shown in Eq. (16).



The sulphate radical anion is a strong oxidant and removes electron from neutral molecules like water and generates hydroxyl radical.



The persulphate ions oxidise the dyes as well as act as electron scavenger. Due to their scavenging property they inhibit e⁻/h⁺ pair recombination at the semiconductor surface [42]. S₂O₈²⁻ ions produce sulphate radical anion (SO₄^{•-}) which in turn produce highly oxidative hydroxyl radicals. These hydroxyl radicals degrade the dyes at a faster rate.

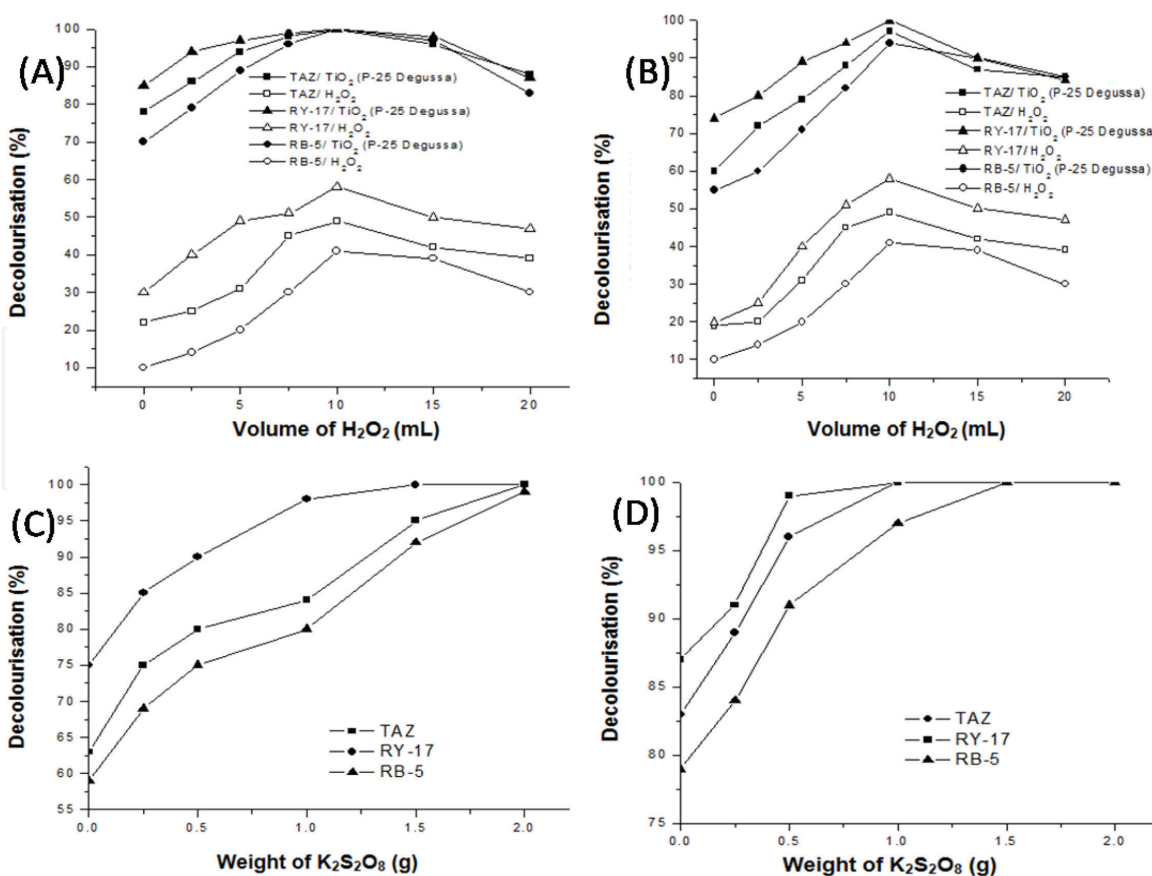


Figure 9.

Effect of (A) H₂O₂ and (B) K₂S₂O₈ on decolourisation of dyes under visible and (C and D) UV irradiations. (reaction conditions: Dye concentration: TAZ = 2×10^{-4} M, RY-17 = 2×10^{-5} M, RB-5 = 2×10^{-5} M, weight of catalyst (P-25 Degussa) = 1.5 g, volume of dye solution = 250 mL, pH = neutral and irradiation time = 7 h).

3.3 Comparison of photocatalytic activities of synthesised TiO₂ with TiO₂ (P-25 Degussa)

The photocatalytic decolourisation of the dyes TAZ, RY-17 and RB-5 were carried out with the synthesised TiO₂ catalyst under the conditions optimised for the best decolourisation with TiO₂ (P-25 Degussa). The optimised conditions for the complete decolourisation of various dyes are given in **Table 4** and the time taken for complete decolourisation of the dyes over the synthesised titania is given in **Table 5**.

Among the three dyes, RY-17 reached complete decolourisation at a shorter irradiation time under both the light sources. RB-5 took longer irradiation time for complete decolourisation. This may be due to its chemical nature (i.e.) RB-5 being diazo dye. Diazo dyes are less degradable than mono azo dye during ozonation [43]. Similar trend of decolourisation was observed with visible light irradiation.

Dye	Initial concentration [M]	pH	Time taken for complete Decolourisation (h)		Weight of catalyst (g) TiO ₂ (P-25 Degussa)
			UV irradiation	Visible irradiation	
TAZ	1×10^{-4}	7	5 ½	6 ½	1.5
RY-17	1×10^{-5}	7	5	6	1.5
RB-5	1×10^{-5}	7	6	7	1.5

Table 4.

The optimised conditions for the complete decolourisation of different dyes using TiO₂ (P-25 Degussa).

Catalyst	Time taken for complete decolourisation (h)					
	TAZ		RY-17		RB-5	
	UV	Visible	UV	Visible	UV	Visible
TiO ₂ (P-25 Degussa)	5½	6½	5	6	6	7
Synthesised TiO ₂	4	3	3½	4	4½	5

Table 5.
Time taken for complete decolourisation (100%) of various dyes using TiO₂ (P-25 Degussa) and synthesised TiO₂.

However, the times at which complete decolourisation took place were different and higher for visible light when compared with UV.

The higher efficiency of the synthesised catalyst when compared to P-25 Degussa may be due to the larger surface area of the synthesised TiO₂ (90.5 m²/g) when compared with TiO₂ (P-25 Degussa) (50 m²/g). Similar type of results was also observed by [44]. Because of the increase in the surface area of synthesised TiO₂ there may be increase in the adsorption of the three dyes.

From the above discussions, it is clear that both degradation and decolourisation of the dyes are highly effective with synthesised TiO₂ compared to TiO₂ (P-25 Degussa) under both the light sources. To further the photocatalytic activity further in the visible region, the modification in the synthesised catalyst has to be carried out by noble metal deposition. Noble metals such as Ag, Au and Pt have been deposited on the synthesised catalyst and they were evaluated for their photocatalytic activity.

3.4 Photodecolourisation studies of metal impregnated titania photocatalysts

To evaluate the photocatalytic activity of noble metal deposited titania catalyst, the decolourisation of dyes (TAZ, RY-17 and RB-5) was carried out under visible and UV light irradiations. The reaction was carried out with 250 mL of dyes of various concentration (TAZ = 1×10^{-4} M, RY-17 and RB-5 = 1×10^{-5} M) and 1.5 g of M/TiO₂ catalyst at neutral pH. The irradiation was carried out by using 125 W low pressure mercury arc lamp (wave length 254 nm) and 85 W tungsten lamp (wave length 365 nm) as UV and visible light sources respectively. The results obtained in the decolourisation of various dyes with M/TiO₂ under UV and visible irradiations are shown in **Figures 10** and **11**.

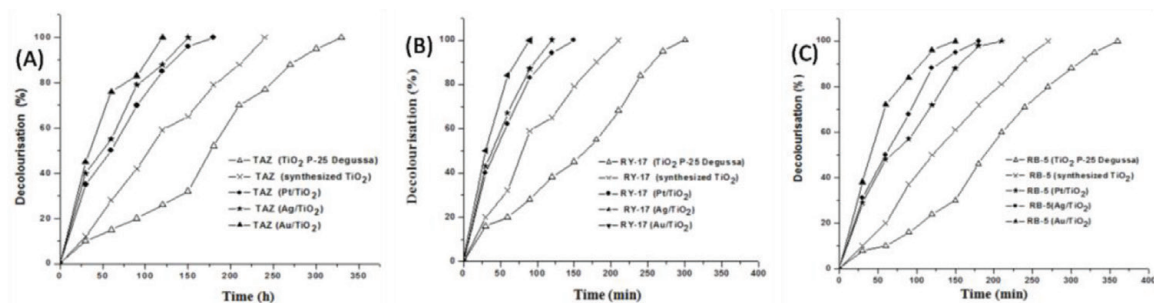
From the above photocatalytic decolourisation studies the following observations were made: Photocatalytic efficiency of the different catalysts for the decolourisation of different dyes were found to be in the following order:

$$\text{Au/TiO}_2 > \text{Ag/TiO}_2 \sim \text{Pt/TiO}_2 > \text{synthesised TiO}_2 > \text{TiO}_2 \text{ (P - 25 Degussa)}$$

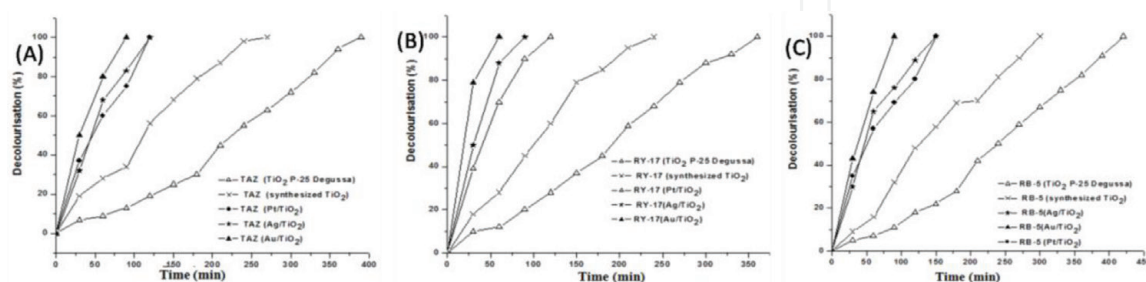
The time at which the complete decolourisation occurred for the different catalysts is given in **Table 6**.

- As far as the decolourisation of the dyes are concerned, all the catalysts found to decolourise RY-17 to the maximum extent followed by TAZ and RB-5.

The percentage decolourisation of different dyes obtained with the different catalysts were determined at the time at which the Au/TiO₂ catalyst showed 100% decolourisation of the respective dyes (TAZ, RY-17 and RB-5) using different catalysts are given in **Table 7**.

**Figure 10.**

Decolourisation of (A) TAZ, (B) RY-17 and (C) RB-5 using different TiO_2 catalysts under UV irradiation. (reaction conditions: Dye concentration: TAZ = 1×10^{-4} M, both RY-17 & RB-5 = 1×10^{-5} M, weight of catalyst = 1.5 g, volume of dye solution = 250 mL and pH = neutral).

**Figure 11.**

Decolourisation of (A) TAZ, (B) RY-17 and (C) RB-5 using different TiO_2 catalysts under visible irradiation. (reaction conditions: Dye concentration: TAZ = 1×10^{-4} M, both RY-17 & RB-5 = 1×10^{-5} M, weight of catalyst = 1.5 g, volume of dye solution = 250 mL and pH = neutral).

Among all the catalysts, M/ TiO_2 catalysts show the higher photocatalytic activity towards the decolourisation of all the three dyes. The higher catalytic activity of M/ TiO_2 catalysts may be due to the smaller band gap values when compared to TiO_2 (P-25 Degussa) and the ability of the noble metals trap the electrons, thus preventing the recombination. The rate constant values obtained with different M/ TiO_2 catalysts in the photocatalytic decolourisation of all the three dyes were found to be highest for Au/ TiO_2 followed by Ag/ TiO_2 and Pt/ TiO_2 . The higher photocatalytic activity of the Au/ TiO_2 catalyst when compared to the other metals is due to the lowered band gap values [45, 46], which leads to the effective absorption of visible light by the catalyst resulting in higher decolourisation.

3.5 Photodegradation studies

The photodegradation studies was carried out with 250 mL of dyes of various concentration (TAZ = 1×10^{-4} M, RY-17 and RB-5 = 1×10^{-5} M) and 1.5 g of M/ TiO_2 catalyst at neutral pH. The irradiation was carried out by using 125 W low pressure mercury arc lamp (wave length 254 nm) and 85 W tungsten lamp (wave length 365 nm) as UV and visible light sources respectively. The degradation was monitored by a TOC analyser and the results are shown in **Figure 12**.

All the above photodegradation experiments show that like photodecolourisation that photodegradation efficiency of all the synthesised catalyst follow similar trend as mentioned below:

- Au/ TiO_2 > Ag/ TiO_2 \approx Pt/ TiO_2 > Synthesised TiO_2 > TiO_2 (P-25 Degussa)
- As far as the dyes are concerned, all the catalysts found to degrade RY-17 to the maximum extent followed by TAZ and RB-5.

Dye	Time taken for complete Decolourisation (h)									
	TiO ₂ (P-25 Degussa)		Synthesised TiO ₂		Pt/TiO ₂		Ag/TiO ₂		Au/TiO ₂	
	UV	Visible	UV	Visible	UV	Visible	UV	Visible	UV	Visible
TAZ	5 ½	6 ½	4	4 ½	3	2	2 ½	2	2	1 ½
RY-17	5	6	3 ½	4	2 ½	2	2	1 ½	1 ½	1
RB-5	6	7	4 ½	5	3 ½	2 ½	3	2 ½	2 ½	1 ½

Table 6.
Time taken for the 100% decolourisation of the dyes (TAZ, RY-17 and RB-5) using different catalysts.

Dye	Decolourisation (%)									
	TiO ₂ (P-25 Degussa)		Synthesised TiO ₂		Pt/TiO ₂		Ag/TiO ₂		Au/TiO ₂	
	UV	Visible	UV	Visible	UV	Visible	UV	Visible	UV	Visible
TAZ	26	16	79	75	79	75	85	83	100	100
RY-17	28	17	83	80	83	80	90	88	100	100
RB-5	24	11	70	72	70	72	88	76	100	100

Table 7.
Percentage decolourisation of the different dyes (TAZ, RY-17 and RB-5) using different catalysts.

The degradation percentage of the dyes (TAZ, RY-17 and RB-5) using different catalysts at the time period of 8 h are given in **Table 8**.

The photocatalytic studies carried out under UV and visible irradiations leads to the following observations:

- The photocatalytic activity of the synthesised catalyst in the decolourisation and degradation of all the dyes was found to be better than TiO₂ (P-25 Degussa) under both UV and visible irradiations.
- Higher percentage of decolourisation and degradation occurred for both TiO₂ (P-25 Degussa) and the synthesised catalyst under UV irradiation when compared to visible irradiation.
- The photocatalytic activities of M/TiO₂ catalysts were found to be higher under both UV and visible irradiations than the synthesised TiO₂.
- The photocatalytic efficiency of the M/TiO₂ was remarkable even under visible light irradiation when compared to the UV irradiation.

The higher activity of M/TiO₂ catalysts under visible region is explained below:

- The activity of noble metals may be attributed to the electronic interaction between the impregnated noble metal and TiO₂. Due to this interaction, Schottky barriers are formed leading to electron hole pair [45].
- The metal deposits traps the electrons and quickly transfers the electrons to oxygen present in the solution to form the highly oxidative O₂^{•-} radical [47].
- The trapping rate of electrons by noble metals is faster rate when compared to the electron transfer from the semiconductor to O₂ [48].

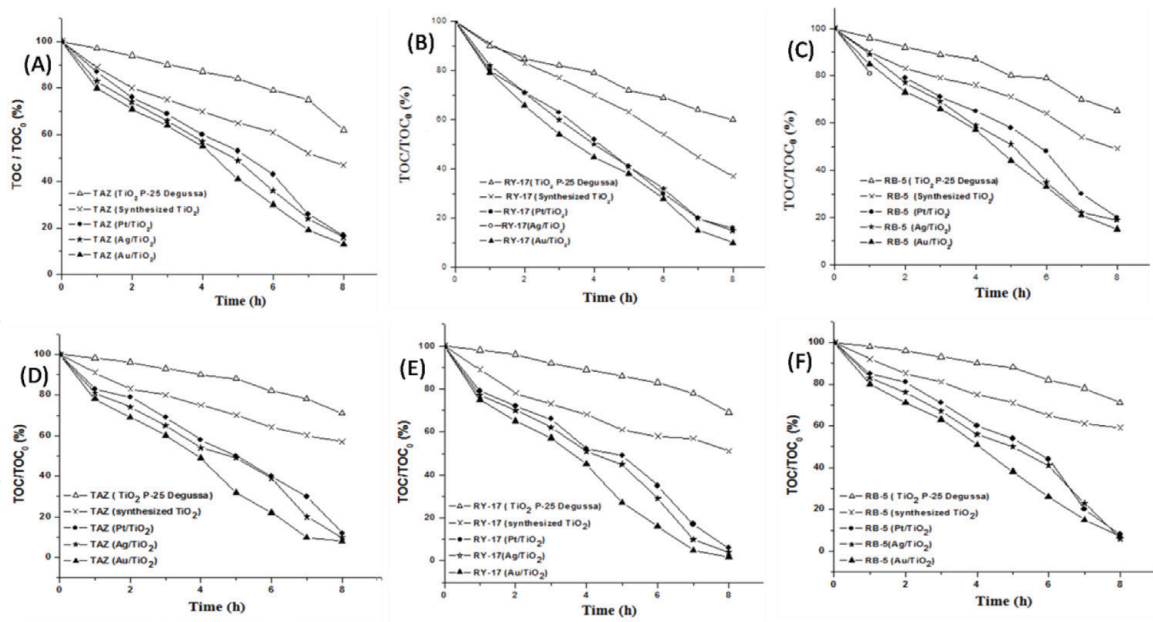


Figure 12. Degradation of (A) TAZ, (B) RY-17 and (C) RB-5 using different TiO₂ catalysts under UV (D,E and F) visible irradiations. (reaction conditions: Dye concentration: TAZ = 1 × 10⁻⁴ M, both RY-17 & RB-5 = 1 × 10⁻⁵ M, weight of catalyst = 1.5 g, volume of dye solution = 250 mL and pH = neutral).

Dyes	Degradation (%)									
	TiO ₂ (P-25 Degussa)		Synthesised TiO ₂		Pt/TiO ₂		Ag/TiO ₂		Au/TiO ₂	
	UV	Visible	UV	Visible	UV	Visible	UV	Visible	UV	Visible
TAZ	38	29	53	43	83	88	84	90	84	90
RY-17	40	31	63	49	84	96	85	96	85	96
RB-5	35	23	51	41	80	82	81	93	81	94

Table 8. Percentage degradation of the dyes (TAZ, RY-17 and RB-5) using different catalysts.

3.6 Effluent studies

3.6.1 Photocatalytic activity of M/TiO₂ with the actual effluent sample

The photocatalytic activity of the synthesised M/TiO₂ catalysts (M = Ag, Au and Pt) was tested with the real effluent samples collected from a textile industry (M/s Ramkay, Erode, Tamil Nadu, India).

The industrial effluent (1 L) sample was first filtered to remove any insoluble matter (carbonates, hydroxides, etc.). As the initial pH was in weakly acidic, it was increased to 7 by adding dil. NH₄OH and the pH adjusted effluent was then subjected to photocatalytic treatment by adding 6 g of the M/TiO₂ (M = Ag, Au and Pt) catalyst. Before the lamp was switched on, the effluent was equilibrated for few minutes with continuous stirring. The effluent was then irradiated using visible light source. Aliquots of the sample were withdrawn at regular time intervals and the extent of decolourisation was monitored using UV-Vis spectrophotometer (Hitachi U 2000). The degradation of the dyes was also determined by using total

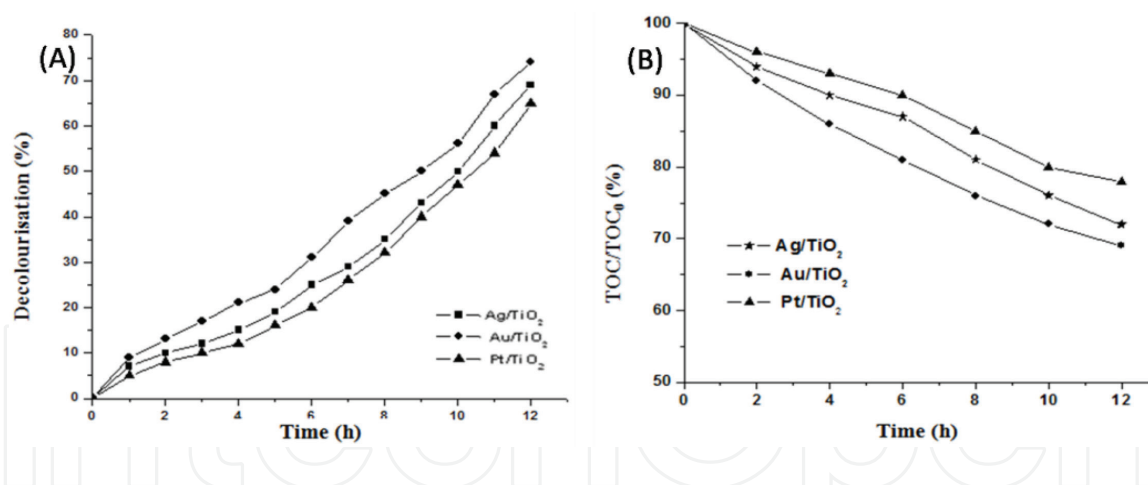


Figure 13.
(A) Decolourisation and (B) degradation of textile effluent using M/TiO₂ catalysts. (reaction conditions: weight of catalyst = 6 g, volume of effluent = 1 L and pH = neutral).

organic carbon analyser (TOC). The decolourisation and degradation results obtained are shown in **Figure 13**.

The effluent studies show that, all the M/TiO₂ catalysts decolourise and degrade the effluent samples significantly. However, these catalysts decolourise the effluent to the extent of only 65–75% and degrade to the extent of 25–30% that too after longer time of irradiation (12 h). The lesser percentages of decolourisation and degradation may be due to the presence of infinite number of dyes, salts etc. in the effluent.

4. Conclusions

The optimised reactions parameters for the degradation of TAT, RY-17 and RB-5 were found to be:

The initial dye concentration (TAZ = 1×10^{-4} M and for both RY-17 and RB-5 = 1×10^{-5} M), catalyst weight (1.5 g/L), pH (7) and the time taken for complete decolourisation (TAZ: 5 ½ h (UV) 6 ½ h (visible), RY-17: 5 h (UV) 6 h (visible), RB-5: 6 h (UV) 7 h (visible)). Decolourisation and degradation were comparatively faster under UV than under visible. Inhibitors such as sodium chloride, sodium carbonate and ethanol decreased the degradation rate and electron acceptors such as H₂O₂ and potassium per sulphate showed beneficial effect. As far as the photocatalytic efficiency of the catalysts are concerned, the following order was observed under both UV and visible irradiations,



Among the noble metals, Au/TiO₂ catalyst was found to be the most active catalyst. This may be attributed to the small band gap value of Au/TiO₂ leading to better visible light absorption.

All the M/TiO₂ catalysts were found to be more active towards the decolourisation of all the dyes even under visible irradiation. The enhanced photocatalytic activity of the M/TiO₂ under visible light irradiation may be due to the presence of impregnated metals, which act as electron traps and by this way they prevent electron hole recombination. The synthesised M/TiO₂ catalysts were found to be very active towards the decolourisation and degradation of textile dye effluent collected from an industry as well.

Acknowledgements

The authors sincerely thank the funding agencies such as MOEF, and DRDO for funding research schemes to Catalysis Laboratory, Applied Sc. And Tech, ACTech, Anna University, Chennai, India.

Conflict of interest

The authors have no conflict of interest.

Author details

Sivakumar Thiripuranthagan* and Valentine Rupa
Department of Applied Science and Technology, Anna University, Chennai, Tamil Nadu, India

*Address all correspondence to: tssivakumar@yahoo.com

IntechOpen

© 2018 The Author(s). Licensee IntechOpen. This chapter is distributed under the terms of the Creative Commons Attribution License (<http://creativecommons.org/licenses/by/3.0>), which permits unrestricted use, distribution, and reproduction in any medium, provided the original work is properly cited. 

References

- [1] Manikavasagam N. Treatment of Textile Processing Effluents. Coimbatore, India: Sakthi Publications; 1995
- [2] Hachem C, Bocquillon F, Zahraa O, Bouchy M. Decolourization of textile industry wastewater by the photocatalytic degradation process. *Dyes and Pigments*. 2001;**49**:117-125. DOI: 10.1016/S0143-7208(01)00014-6
- [3] Bickley RI, Carreno TG, Lees JS, Palmisano L, Tilley RJD. A spectral investigation of titanium dioxide photocatalysts. *Journal of Solid State Chemistry*. 1992;**92**:178-190. DOI: 10.1016/0022-4596(91)90255-G
- [4] Linsebigler AL, Lu G, Yates JT. Photocatalysis on TiO₂ surfaces: Principles, mechanisms, and selected results. *Chemical Reviews*. 1995;**5**: 735-758. DOI: 10.1021/cr00035a013
- [5] Howe RF. Recent developments in photocatalysis. *Developments in Chemical Engineering and Mineral Processing*. 1998;**6**(1):55-84. DOI: 10.1002/apj.5500060105
- [6] Renault NJ, Pichat P, Foissy A, Mercier R. Study of the effect of deposited platinum particles on the surface charge of titania aqueous suspensions by potentiometry, electrophoresis, and labeled-ion adsorption. *The Journal of Physical Chemistry*. 1986;**90**:2733-2738. DOI: 10.1021/j100403a035
- [7] Hadjiivanov KI, Klissurski DG. Surface chemistry of titania (anatase) and titania-supported catalysis. *Chemical Society Reviews*. 1996:61-69. DOI: 10.1039/CS9962500061
- [8] Sanchez E, Lopez T. Effect of the preparation method on the band gap of titania and platinum-titania sol-gel materials. *Materials Letters*. 1995;**25**:271-275. DOI: 10.1016/0167-577X(95)00190-5
- [9] Yang JC, Kim YC, Shul YG, Shin CH, Lee TK. Characterization of photoreduced Pt/TiO₂ and decomposition of dichloroacetic acid over photoreduced Pt/TiO₂ catalysts. *Applied Surface Science*. 1997;**121**:525-529. DOI: 10.1016/S0169-4332(97)00359-0
- [10] Moore WA, Kroner RC, Ruchhoft CC. Dichromate reflux method for determination of oxygen consumed. *Analytical Chemistry*. 1949;**21**(8): 953-957. DOI: 10.1021/ac60032a020
- [11] Dobbs RA, Williams RT. Elimination of chloride interference in the chemical oxygen demand test. *Analytical Chemistry*. 1963;**35**(8):1064-1067. DOI: 10.1021/ac60201a043
- [12] Lee BY, Park SH, Kang M, Lee SC, Choung SJ. Preparation of Al/TiO₂ nanometer photocatalyst film and the effect of H₂O addition on photocatalytic performance for benzene removal. *Applied Catalysis A: General*. 2003;**253**:371-380. DOI: 10.1016/S0926-860X(03)00542-8
- [13] Wang C, Liu C, Zheng X, Chen J, Shen T. The surface chemistry of hybrid nanometer sized particles 1. Photodeposition of gold on ultrafine TiO₂ particles. *Colloids and Surfaces, A: Physicochemical and Engineering Aspects*. 1998;**131**:271-280
- [14] Hahakura S, Isoda S, Ogawa T, Moriguchi S, Kobayashi T. Formation of ultrafine platinum particles in an aqueous solution with a surfactant. *Journal of Crystal Growth*. 2002;**237-239**(3):1942-1945
- [15] Sobana N, Muruganandham M, Swaminathan M. Nano Ag particle doped TiO₂ for efficient photodegradation of direct azo dyes. *Journal of Molecular Catalysis*.

2006;**258**:124-132. DOI: 10.1016/j.molcata.2006.05.013

[16] Reddy EP, Davydov L, Smirniots P. Characterization of titania loaded V-, Fe-, and Cr- incorporated MCM-41 by XRD, TPR, UV-Vis, Raman and XPS techniques. *The Journal of Physical Chemistry. B.* 2002;**106**:3394-3401. DOI: 10.1021/jp013898

[17] Sakthivel S, Shankar MV, Palanichamy M, Arabindoo B, Bahnemann DW, Murugesan V. Enhancement of photocatalytic activity by metal deposition: Characterisation and photonic efficiency of Pt, Au and Pd deposited on TiO₂ catalyst. *Water Research.* 2004;**38**(13):3001-3008. DOI: 10.1016/j.watres.2004.04.046

[18] Wei TY, Wan CC. Heterogeneous photocatalytic oxidation of phenol with titanium dioxide powders. *Industrial and Engineering Chemistry Research.* 1991;**30**:1293-1300. DOI: 10.1021/ie00054a033

[19] Wang KS, Chen HY, Huang LC, Su YC, Chang SH. Degradation of reactive black 5 using combined electrochemical degradation-solar-light/immobilized TiO₂ film process and toxicity evaluation. *Chemosphere.* 2008;**72**(2):299-305

[20] Matthews RW. Hydroxylation reactions induced by near-ultraviolet photolysis of aqueous titanium dioxide suspensions. *Journal of the Chemical Society, Faraday Transactions.* 1984;**80**:457-471. DOI: 10.1039/F19848000457

[21] Okamoto KI, Yamamoto Y, Tanaka H, Tanaka M. Heterogeneous photocatalytic decomposition of phenol over TiO₂ powder. *Bulletin of the Chemical Society of Japan.* 1985;**58**:2015-2022

[22] Okamoto KI, Yamamoto Y, Tanaka H, Tanaka M. Kinetics

of heterogeneous photocatalytic decomposition of phenol over anatase TiO₂ powder. *Bulletin of the Chemical Society of Japan.* 1985b;**58**:2023-2028

[23] Rideh L, Wehrer A, Ronze D, Zoulalian A. Photocatalytic degradation of 2-chlorophenol in TiO₂ aqueous suspension : Modeling of reaction rate. *Industrial and Engineering Chemistry Research.* 1997;**36**:4712-4718

[24] Matthews RW. Photooxidation and adsorption of methylene blue on thin films of near-ultraviolet-illuminated TiO₂. *Journal of the Chemical Society, Faraday Transactions.* 1989;**1**, **85**(6):1291-1302. DOI: 10.1039/F19898501291

[25] Davis RJ, Gainer JL, Neal GO, Wenwu I. Photocatalytic decolourisation of wastewater dyes. *Water Environment Research.* 1994;**66**:50-53. DOI: 10.2175/WER.66.1.8

[26] Rao KVS, Lavédrine B, Boule P. Influence of metallic species on TiO₂ for the photocatalytic degradation of dyes and dye intermediates. *Journal of Photochemistry and Photobiology A: Chemistry.* 2003;**154**(2-3):189-193. DOI: 10.1016/S1010-6030(02)00299-X

[27] Suri RPS, Liu J, Hand DW, Crittenden JC, Perram DL, Mullins ME. Heterogeneous photocatalytic oxidation of hazardous organic contaminants in water. *Water Environment Research.* 1993;**65**:665-673

[28] Chen JR, Xu XW, Lee AS, Yen TFA. Feasibility study of dechlorination of chloroform in water by ultrasound in the presence of hydrogen peroxide. *Environmental Technology.* 1990;**11**:829-836. DOI: 10.1080/09593339009384930

[29] Stumm W, Morgan JJ. *Aquatic Chemistry.* New York: John Wiley and Sons; 1981

- [30] Hidaka H, Nohara K, Zhao J. Photo-oxidative degradation of the pesticide permethrin catalysed by irradiated TiO₂ semiconductor slurries in aqueous media. *Journal of Photochemistry and Photobiology A: Chemistry*. 1992a;**64**:247-253. DOI: 10.1016/1010-6030(92)85111-7
- [31] Hidaka HJ, Zhao J, Pelizzetti E, Serpone N. Photodegradation of surfactants 8. Comparison of photocatalytic process between anionic sodium dodecyl benzene sulfonate and cationic benzyl dodecyl dimethyl ammonium chloride on the TiO₂ surface. *The Journal of Physical Chemistry*. 1992b;**96**:2226-2229
- [32] Zhao J, Wu T, Wu K, Oikawa K, Hidaka H, Serpone N. Photoassisted degradation of dye pollutants. Degradation of the cationic dye Rhodamine B in aqueous anionic surfactant/TiO₂ dispersions under visible light irradiation: Evidence for the need for substrate adsorption TiO₂ particles. *Journal of Environmental Science and Technology*. 1998;**32**: 2394-2401. DOI: 10.1021/es9707926
- [33] Kormann C, Bahnemann DW, Hoffmann MR. Photolysis of chloroform and other organic molecules in aqueous TiO₂ suspensions. *Environmental Science & Technology*. 1991;**25**:494-500. DOI: 10.1021/es00015a018
- [34] Mansila HD, Villaseñor J, Maturana G, Baeza T, Freer J, Dural N. ZnO-catalysed photodegradation of Kraft black liquor. *Journal of Photochemistry and Photobiology A: Chemistry*. 1994;**78**:267-273. DOI: 10.1016/1010-6030(93)03731-U
- [35] Nasr C, Vinodgopal K, Hotchandani S, Chattopadhyay AK, Kamat PV. Photocatalytic reduction of azo dyes naphthol blue black and disperse blue 79. *Research on Chemical Intermediates*. 1997;**23**:219-231
- [36] Low GKC, Mcevoy SR, Matthews RW. Formation of ammonium and nitrate ions from photocatalytic oxidation of ring nitrogenous compounds over titanium dioxide. *Chemosphere*. 1989;**19**:1611-1623
- [37] Nohara K, Hidaka H, Pelizzetti E, Serpone N. Processes of formation of NH₄⁺ and NO₃ ions during the photocatalysed oxidation of N-containing compounds at the titania/water interface. *Journal of Photochemistry and Photobiology A: Chemistry*. 1997;**102**:265-272. DOI: 10.1016/S1010-6030(96)04478-4
- [38] Muneer M, Bahnemann D. Semiconductor mediated photocatalysed degradation of two selected pesticide Terbacil and 2, 4, 5, Tribromoimidazole. *Water Science and Technology*. 2001;**4**:331-337
- [39] Sokmen M, Ozkan A. Decolourising textile wastewater with modified titania: The effects of inorganic anions on the photocatalysis. *Journal of Photochemistry and Photobiology A: Chemistry*. 2002;**147**:77-81. DOI: 10.1016/S1010-6030(01)00627-X
- [40] Nevim S, Arzu H, Gulın K, Cinar Z. Prediction of primary intermediates and the photodegradation kinetics of 3-aminophenol in aqueous TiO₂ suspensions. *Journal of Photochemistry and Photobiology A: Chemistry*. 2001;**139**:225-232. DOI: 10.1016/S1010-6030(01)00368-9
- [41] Galindo C, Kalt A. UV-H₂O₂ oxidation of monoazo dyes in aqueous media: A kinetic study. *Dyes and Pigments*. 1999;**40**(1):27-35. DOI: 10.1016/S0143-7208(98)00027-8
- [42] Pelizzetti E, Schiavello M. *Photochemical Conversion and Storage of Solar Energy*. Kluwer Acad. Publ. Dordrecht; 1991
- [43] Shu HY, Huang CR. Degradation of commercial azo dyes in water

using ozonation and UV enhanced ozonation process. *Chemosphere*. 1995;**31**(8):3813-3825. DOI: 10.1016/0045-6535(95)00255-7

[44] Sivalingam G, Nagaveni K, Hegde MS, Madras G. Photocatalytic degradation of various dyes by combustion synthesized nano anatase TiO₂. *Applied Catalysis B: Environmental*. 2003;**45**:23-28. DOI: 10.1016/S0926-3373(03)00124-3

[45] Herrmann JM, Disdier J, Pichat P. Photoassisted platinum deposition on TiO₂ powder using various platinum complexes. *The Journal of Physical Chemistry*. 1986;**90**:6028-6034. DOI: 10.1021/j100280a114

[46] Yuexiang L, Gongxvan L, Shuben L. Photocatalytic transformation of rhodamine B and its effect on hydrogen evolution over Pt/TiO₂ in the presence of electron donors. *Journal of Photochemistry and Photobiology A: Chemistry*. 2002;**152**:219-228. DOI: 10.1016/S1010-6030(02)00210-1

[47] Vamathevan V, Amal R, Beydoun D, Low G, Mc Evoy S. Photocatalytic oxidation of organics in water using pure and silver-modified titanium dioxide particles. *Journal of Photochemistry and Photobiology A: Chemistry*. 2002;**148**:233-245. DOI: 10.1016/S1010-6030(02)00049-7

[48] Vorontsov AV, Savinov EN, Jin ZS. Influence of the form of photodeposited Pt on titania upon its photocatalytic activity in CO and acetone oxidation. *Journal of Photochemistry and Photobiology A: Chemistry*. 1999;**125**:113-117. DOI: 10.1016/S1010-6030(99)00073-8